

Online Research @ Cardiff

This is an Open Access document downloaded from ORCA, Cardiff University's institutional repository: <https://orca.cardiff.ac.uk/id/eprint/137920/>

This is the author's version of a work that was submitted to / accepted for publication.

Citation for final published version:

Lomelí-Rodríguez, Mónica, Martín-Molina, Miguel, Jiménez-Pardo, María, Nasim-Afzal, Zahara, Cauët, Solène I., Davies, Thomas E., Rivera-Toledo, Martín and Lopez-Sanchez, Jose A. 2016. Synthesis and kinetic modeling of biomass-derived renewable polyesters. *Journal of Polymer Science Part A: Polymer Chemistry* 54 (18) , pp. 2876-2887. 10.1002/pola.28173 file

Publishers page: <http://dx.doi.org/10.1002/pola.28173>
<<http://dx.doi.org/10.1002/pola.28173>>

Please note:

Changes made as a result of publishing processes such as copy-editing, formatting and page numbers may not be reflected in this version. For the definitive version of this publication, please refer to the published source. You are advised to consult the publisher's version if you wish to cite this paper.

This version is being made available in accordance with publisher policies.

See

<http://orca.cf.ac.uk/policies.html> for usage policies. Copyright and moral rights for publications made available in ORCA are retained by the copyright holders.



Synthesis and Kinetic Modeling of Biomass-Derived Renewable Polyesters

Mónica Lomelí-Rodríguez,¹ Miguel Martín-Molina,¹ María Jiménez-Pardo,¹
Zahara Nasim-Afzal,¹ Solène I. Cauët,¹ Thomas E. Davies,¹ Martín Rivera-Toledo,²
Jose A. Lopez-Sanchez¹

¹Stephenson Institute for Renewable Energy, Department of Chemistry, University of Liverpool, Crown Street, Liverpool, L69 7ZD, United Kingdom

²Departamento De Ingeniería Y Ciencias Químicas, Universidad Iberoamericana, Prolongación Paseo De La Reforma 880, Ciudad De México, México, 01210

Correspondence to: J. A. Lopez-Sanchez (E-mail: jals@liv.ac.uk)

Received 17 February 2016; accepted 9 May 2016; published online 13 July 2016

DOI: 10.1002/pola.28173

ABSTRACT: The biomass-derived polyesters poly(1,3-propylene 2,5-furandicarboxylate) (PPF), poly(1,3-propylene succinate) (PPS) and poly(1,3-propylene 2,5-furandicarboxylate-co-1,3-propylene succinate) (PPFPS) have been synthesized *via* a two-step process involving polycondensation and azeotropic distillation. The kinetic parameters were obtained by fitting the experimental data from a batch polymerization reactor to three different kinetic models for polyesterification reactions. The activation energies of the all monomer systems were obtained by Arrhenius plots. Given the increasing availability of biomass-derived monomers their use in renewable polyesters as substitutes for fossil fuel derived chemicals becomes a distinct possi-

bility. The kinetic modeling of the uncatalyzed polyesterification reactions will enable further integrative process simulation of the studied bioderived polymers and provide a reference for future practical study or industrial applications of catalyzed polyesterification reactions and other bioderived monomer systems. © 2016 The Authors. Journal of Polymer Science Part A: Polymer Chemistry Published by Wiley Periodicals, Inc. J. Polym. Sci., Part A: Polym. Chem. **2016**, 54, 2876–2887

KEYWORDS: 2,5-furandicarboxylic acid; biomass-derived polymer; renewable polymer; polyesters; succinic acid

INTRODUCTION The twentieth century industry was defined by widespread production of fuels, polymers, pharmaceuticals, solvents, fertilizers, and other commodities from traditional fossil reservoirs.¹ One of the greatest challenges of the twenty-first century is the development of bio-based processes and materials synthesized from renewable and sustainable resources. This is because of the rapid oil feedstock depletion and the negative environmental consequences of its use.² The polymer industry is likely to require moving toward more sustainable processes to lower its dependence on petrochemical sources and, will benefit from complementing or improving existing materials thanks to a range of new bio-derived monomers. The wide variety of polyester applications, from packaging and textiles to healthcare appliances and automotive, represent an exciting area for renewable bio-derived feedstock to be considered.³ Polyesters are mainly produced by the equilibrium condensation reaction between a dicarboxylic acid and a diol; or alternatively, using the methyl ester of the acid instead, releasing methanol as a

by-product. In particular, poly(ethylene terephthalate) (PET), is synthesized in a two-step process, involving first the formation of a precursor from dimethyl terephthalate and ethylene glycol at high temperature followed by the polymerization of the precursor.⁴ Commonly used monomers for polyesters include terephthalic acid, isophthalic acid, maleic anhydride, adipic acid, ethylene glycol, 1,4-butanediol, and neopentyl glycol, among others. The emerging bioeconomy and the development of improved routes to bioderived chemicals from biomass, is offering the opportunity to source several biobased diols and diacids as replacements to the oil-derived ones, which are potential candidates for polyester synthesis leading to the formation of new polymeric materials. In particular, our group is focusing on the study of carbohydrate-derived diols along with diacids such as succinic acid (SA) and 2,5-furandicarboxylic acid (FDCA).

1,3-Propanediol (PDO) is obtained in a two-step process: yeast fermentation to glycerol followed by the bacterial

Additional Supporting Information may be found in the online version of this article.

This is an open access article under the terms of the Creative Commons Attribution License, which permits use, distribution and reproduction in any medium, provided the original work is properly cited.

© 2016 The Authors. Journal of Polymer Science Part A: Polymer Chemistry Published by Wiley Periodicals, Inc.

transformation to PDO.⁵ An improved one-step biological production of PDO from a fermentable carbon source by a single microorganism has been patented by Dupont and Tate & Lyle BioProducts resulting in the commercial petroleum-free biobased glycol SusterraTM.⁶ In the case of diacids, SA has been widely reported for the synthesis of polyesters and can be bioderived *via* fermentation under mild conditions,⁷ replacing the conventional synthesis *via* catalytic hydrogenation of maleic acid. The bio-derived diacid monomer with the most potential in the polymer market is FDCA, which is a high value derivative from hydroxymethyl furfural, itself an important chemical platform obtained from the dehydration of C₅ and C₆ sugars.⁸ FDCA can be produced by the selective oxidation of hydroxymethyl furfural (HMF) with a wide variety of heterogeneous catalysts.^{9–14} The production of FDCA from the oxidation of HMF with a metal permanganate in an alkaline media has also been patented by Canon.¹⁵ FDCA is envisioned as a replacement for terephthalic acid in the synthesis of PET and PBT (poly(butylene terephthalate)),¹⁶ and has already been patented for the production of poly(ethylene 2,5-furandicarboxylate) (PEF) and poly(butylene 2,5-furandicarboxylate) (PBF).¹⁷ Starting with the early work of Moore,¹⁸ FDCA has been the subject of extensive research over the last years with a drive to develop it as a green chemical building block for polyesters.^{19–24} However, despite the current growth of the research and applications of biomass derived polyesters, both kinetic data and process modeling for the polymerization of biosourced monomers are scarce. The foundations of general step-growth polymerization kinetics were firstly established by Flory²⁵ and then extended by Szabo-Rethy²⁶ by considering the effect of the water released during the polyesterification reaction. Several authors have proposed kinetic and reactor models for well-established systems such as PET,^{27–30} maleic anhydride and 1,2-propanediol^{31–33} or using phthalic anhydride instead of the diacid.^{34,35} In the 1980s, a comprehensive review of general polyesterification models and kinetic data was compiled by Fradet and Maréchal including kinetic expressions for both non-catalyzed and catalyzed polyesterifications.³⁶ It includes a great compendium of solvents, monomers and reaction conditions, as well as the main techniques utilized in polyesterification kinetic studies. More recently, the integration of modeling step-growth polymerization and product design toward an optimized polymer manufacturing process was reviewed by Seavey and Liu.³⁷ For bio-based monomers there are a number of studies covering succinic acid with ethylene glycol, butanediol or hexanediol and studies of FDCA with ethylene glycol and butanediol. Bikiaris *et al.* performed the mathematical modeling of the esterification of succinic acid polyesters.³⁸ In another study, they reported reference activation energies for poly(1,3-propylene succinate) with values of 52 kJ mol^{−1} for the esterification step and 68.3 kJ mol^{−1} for the transesterification with k_2 values of $26\text{--}47 \times 10^{-4}$ (kg/meq) h^{−1} at 210–230 °C.³⁹ Comparatively the activation energy for poly(butylene succinate) was reported by Park *et al.* as 149 kJ mol^{−1} with K_{app} $0.33\text{--}1.90 \times 10^{-2}$ (L²/mol²) min^{−1} at 170–190 °C.⁴⁰ Catalyzed reactions have also been studied primarily with titanium (IV) tetrabutoxide as catalyst. Garin *et al.* looked at the kinetics of poly(-

butylene succinate) synthesis with and without catalyst.⁴¹ Hu reported the polycondensation kinetics of aliphatic-aromatic copolyesters comprising succinic acid, terephthalic acid, and 1,4-butanediol catalyzed by titanium butoxide.⁴² The pseudo first-order reaction polymerization of ethylene glycol and 1,4-butanediol with FDCA was reported by J. Ma *et al.*²³ The activation energy for PEF is reported as 184.3 kJ mol^{−1} for the esterification step and 163.4 kJ mol^{−1} for the polycondensation step.⁴³ In this work, we report the synthesis of the following biomass derived polyesters: PPF (poly(1,3-propylene 2,5-furandicarboxylate)), PPS (poly(1,3-propylene succinate)) and PPFPS poly(1,3-propylene 2,5-furandicarboxylate-co-1,3-propylene succinate)) and their kinetic parameters obtained by fitting the experimental data from a batch polymerization reactor to three different kinetic mechanisms for polyesterification reactions. The effect of temperature and molar ratio of reactants is also examined and discussed. This modeling will enable further development of polyesterification process simulation.

EXPERIMENTAL

Materials

2,5-Furandicarboxylic acid (FDCA, >98%) was purchased from Manchester Organics Ltd. Succinic acid (SA, >99%), was purchased from Sigma Aldrich. Renewably sourced 1,3-propanediol SusterraTM was kindly provided by DuPont Tate & Lyle BioProducts. All other chemicals were of analytical grade.

Synthesis of Biomass-Derived Polyesters

Polymerization reactions were performed in a five-neck round-bottom flask (250 mL) or a single wall glass reactor (500 mL) with a five-neck lid. The reactor was fitted with an overhead stirrer, thermocouple, sampling port, a Raschig-ring packed column and a distillation condenser (Fig. 2). Nitrogen was bubbled continuously through a gas inlet to ensure the removal of water and an inert system. The reactor was heated with a heating mantle from ElectrothermalTM (CMU0500/CE, 280 W) and the temperature was monitored through a digital temperature controller (MC810B) coupled to the mantle, Supporting Information Figure S1.

The synthesis was performed following a two-stage process: esterification and polycondensation. First, the required amounts of monomers were charged into the reactor: FDCA (~30–160 g), SA (~30–100 g) and PDO (~80–160 g) prior to heating and stirring. In the case of the copolyesters, FDCA and the diol were mixed first and heated to 150 °C, followed by the addition of succinic acid.

The reactor was then heated up to 210–230 °C according to each particular reaction and continuously stirred at 350 rpm. The temperature at the condenser head remained in the range of 95–100 °C while the reaction water was monitored and driven off *via* the condenser. The esterification reaction was completed after all the water had been removed and the head temperature was back to ambient temperature. The polycondensation reaction was continued by azeotropic distillation adding 3 wt% xylene as azeotropic

agent under atmospheric pressure for several hours to increase the molecular weight and remove residual diol. Upon addition of xylene a drop of temperature of up to 15 °C occurred and the mixture returned to the desired process temperature within a few minutes. The polymerization was monitored regularly by acid value determination as described below. When an acid value below 10 mg KOH/g polyester was reached, the reaction was cooled down. PPS, PPFPS 15/85 and 30/70 polymers were obtained as yellow to dark yellow liquids and PPFPS 50/50 to 85/15 and PPF as light brown powders prior to purification, Supporting Information Figure S2. Purification method is available in Supporting Information.

A number of polymerizations were run in duplicates to check the reproducibility of acid value data and variation of kinetic parameters. Table of acid values and calculated kinetic parameters for some of these duplicate runs can be found in Supporting Information Tables S6 and S7.

Polyester Characterization

Acid Value Determination

The concentration of dicarboxylic acid (acid value, AV) was determined by titration. A known amount of sample was dissolved in 50 mL of a 50:50 (v/v) solution of methanol and xylene and titrated with potassium hydroxide (KOH) 0.1 M using phenolphthalein as indicator (eq 1).

$$AV = \frac{\text{Titre volume (mL)} \times 56.1 \times 0.1}{\text{Sample weight (g)}} \quad (1)$$

where 56.1 is the molecular weight of KOH (g/mol) and 0.1 is the molar concentration of KOH.

Nuclear Magnetic Resonance Spectroscopy

Nuclear magnetic resonance spectroscopy (^1H NMR) measurements were performed on a Bruker NMR spectrometer (400 MHz). Deuterated chloroform (CDCl_3) was used as solvent for all samples.

Gel Permeation Chromatography

Gel permeation chromatography (GPC) was carried out on an Agilent 1260 Infinity with two Agilent ResiPore Organic 250 \times 4.6 mm columns, a guard column and a refractive index detector. The eluent was tetrahydrofuran (THF) at a flow rate of 0.3 mL min^{-1} . Molecular weights were calculated using a conventional calibration with Polystyrene standards.

Modeling and Parameter Optimization

The adjustable parameters of the model were estimated by fitting the experimental acid conversion time data over the entire conversion range under different reaction conditions. The solutions for each model are based on sets of ordinary differential equations (ODE) defined by the reaction rate laws, following a Runge-Kutta method. The commercial software MatlabTM was used for all simulations and parameter optimization. The objective function is expressed as in eq 2:

$$\text{Min } Z = \sum_{j_p}^{N_p} (C_i - C_{i(p)})^2 \quad (2)$$

Where Z is the sum over all N_p data points of the squared difference between the model predictions $C_{i(p)}$ and the measurement C_i , and y_p is the set of kinetic parameters to be estimated, which refers to the kinetic rate constants and activation energies from the ODE system, which will be shown in the next section.

Polyesterification Kinetic Simulation

Three different reaction models reported in the literature for polyesterification were tested to simulate the biobased polyesters synthesized while enabling the calculation of reaction parameters, such as kinetic coefficients and activation energies.

Model 1: Flory-Derived Model

In this model, the overall kinetic rate of the uncatalysed polycondensation reaction can be estimated through the calculation of the concentration of the carboxylic groups present. The model assumes that the overall rate coefficient k is independent of the molecular size.⁴⁴ Thus, the reaction rate is defined as the decay of COOH groups concentration (C) with respect to time:

$$r = -\frac{d[C]}{dt} \quad (3)$$

In his studies, Flory determined that self-catalyzed polyesterification rate is second order for diacid and first-order for diol.²⁵ It is also considered that any water produced is immediately removed and that reverse reaction of hydrolysis is negligible. The reaction rate equation is therefore defined by:

$$-\frac{d[C]}{dt} = k[C]^2[\text{OH}] \quad (4)$$

Where $[\text{OH}]$ refers to the hydroxyl group concentration.

Assuming stoichiometric amounts of diol and diacid as well as equal rate of consumption of hydroxyl and carboxylic acid groups, the rate expression becomes:

$$-\frac{d[C]}{dt} = k[C]^3 \quad (5)$$

Integration of the differential equation leads to eq 6:

$$\frac{1}{[C]^2} = \frac{1}{[C]_0^2} + 2kt \quad (6)$$

The previous expression refers particularly to a third order reaction. Studies following Flory have demonstrated that the order of self-catalysed or uncatalysed polyesterification varied during the polymerization with changed in the reaction medium. Thus, we chose a general equation for a two monomer system, considering equal reactivity of the reactants and the n^{th} reaction order, defined as follows:

$$(n-1)k_n t = \frac{1}{C_0^{n-1}} - \frac{1}{C_0^{n-1}} \quad (7)$$

where C_0 is the concentration of carboxylic groups at time $t = 0$, C is the concentration of carboxylic group at time t and k is the kinetic coefficient of the n^{th} order reaction.

Instead of the concentration, Flory²⁵ introduced the degree of polycondensation (P), which is defined as eq 8:

$$P = \frac{C_0 - C}{C_0} \quad (8)$$

Substituting this expression into eq 7 leads to:

$$(n-1)k_n t = \frac{1}{((C_0(1-P))^{n-1}} - \frac{1}{C_0^{n-1}} \quad (9)$$

Model 2: Non-Stoichiometric Balance of Reactants

In this model, deviation from stoichiometry of diol:diacid ratio and changes in the mass of polymerization mixture because of the loss of water are incorporated in the reaction rate equation. Model 2 follows the rate equation reported by Fradet and Maréchal³⁶ for self-catalyzed, non-equimolar polyesterifications and is defined by eq 10:

$$\frac{dC}{dt} = -kC^m \left[C + b_0 \left(\frac{1 - 0.018C}{1 - 0.018C_0} \right) \right]^n \quad (10)$$

Where k is the reaction rate coefficient, m is the reaction order with respect to the acid, n is the reaction order with respect to the diol, and b_0 is the algebraic excess of the hydroxyl group concentration at the beginning of the reaction. The factor of 0.018 accounts for the water released, as previously described in the Szabo-Rethy correction.²⁶ Full description of the development of the rate equation is available in Supporting Information, eqs S1–S9.

Model 3: Chen and Wu Model

In this Model Chen and Wu⁴⁵ assumed that changes in the dielectric constant of the polymerization medium during polymerization influenced the probability of ion-pair formation, first step of the self-catalysed polyesterification mechanism, Supporting Information Figure S4. The assumption is that the probability of ion-pair formation goes up with decreasing dielectric constant of the medium. They also assumed that all water is not removed from the polyesterification medium and that the hydrolysis of the ester should be taken into account.

The ordinary differential equation below (eq 11) was reported by Nalampang,³⁵ and improves upon the original model published by Chen and Wu⁴¹ for the modeling of the uncatalyzed reaction between maleic anhydride, phthalic anhydride, and 2-methyl-1,3-propanediol:

$$\frac{dp}{dt} = kK_{e0}e^{xp}COOH_0^2(1-p)^2(r-p) - k_h[H_2O]p \quad (11)$$

Where k is the polyesterification rate constant ($\text{kg mol}^{-1} \text{min}^{-1}$), k_h is the rate constant for hydrolysis of

TABLE 1 Reaction Conditions for Biomass Derived Polyester Synthesis

Polyester	Temp. (°C)	Molar Ratio Diol:Diacid	FDCA (% mol)	SA (% mol)
PPS	210–230	1.1	0	100
PPFPS 15/85	210–230	1.5	15	85
PPFPS 30/70	210–230	1.5	30	70
PPFPS 50/50	210–230	1.5	50	50
PPFPS 70/30	210–230	1.5	70	30
PPFPS 85/15	210–230	1.5	85	15
PPF	210–230	1.6	100	0

ester bonds ($\text{kg mol}^{-1} \text{min}^{-1}$), K_{e0} is the equilibrium ionization constant at zero fractional conversion (p) (kg mol^{-1}), and the term $\exp(xp)$ accounts for the increase in K_{e0} with the decrease of the electric constant with increasing p . The term r refers to the mol ratio of diol to diacid at the beginning of reaction, defined as $[OH]_0/[COOH]_0$. Nalampang *et al.* chose to use a value for α of 0.61 for self-catalyzed polycondensations based on Chen and Wu's work with fitted parameter α ranging from 0.23 to 0.61 depending on reaction conditions. In the present work, this term will be fitted along with the rate and equilibrium ionization coefficients.

RESULTS AND DISCUSSION

In the following sections we report a range of bioderived polyesters synthesized at different temperatures and monomer ratios, and their kinetic modeling calculated following the three polyesterification models—Models 1, 2 and 3 as described in the previous section.

Experimental Development

The reaction conditions for the synthesis of the biopolyesters (PPF, PPS, and PPFPS) are summarized in Table 1 and their structures in Figure 1. Successful polymerization and copolymerization of FDCA was obtained following some method development. The process temperatures were chosen according to our experience and published results on the processing of FDCA polymerization; knowing that above 230 °C gelation is promoted and Acid Value measurements are difficult and below 210 °C full dissolution of FDCA i.e. the clear point, could not be reached.

Optimal diol:diacid ratio was determined through an iterative process. Polymerizations were carried out at 220 °C starting at a diol:diacid molar ratio of 5:1, going down to 3:1, 2:1, 1.8:1 and finally 1.6:1. At this ratio the clear point could be reached in approximately 3 hours and the reaction mixture was processable. This ratio is in agreement with the results reported by Jiang *et al.*²¹ In polymerization attempts with a diol:diacid molar ratio of 1.3:1, FDCA did not dissolve and the reaction mixture was a white paste that would burn under heating rather than polymerize.

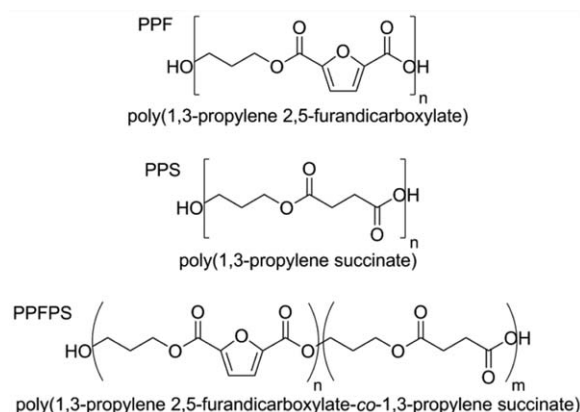


FIGURE 1 Chemical structures of the biomass derived polyesters synthesized.

We also found that proper dispersing of the FDCA powder is crucial to avoid the formation of hot spots. When all reagents were added together, areas of high FDCA concentration would form in the early stages of the polymerization at the bottom of the reactor where mixing was insufficient. We found that a preliminary step of mechanical mixing of the diol and 2,5-furandicarboxylic acid followed by heating before the addition of succinic acid overcame the diffusion limitation provoked by the poor solubility of FDCA. We believe that this experimental procedure was determinant in obtaining robust and reproducible polymerization data.

During these preliminary studies it was found that special considerations did not need to be applied for the succinic acid-rich systems. Tests showed that polymerization mixtures were still processable with a diol to succinic acid ratio as

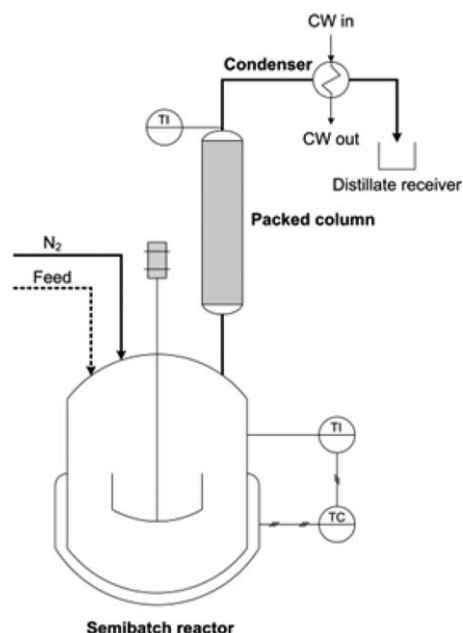


FIGURE 2 Diagram of semi batch reactor used for polymerization reactions.

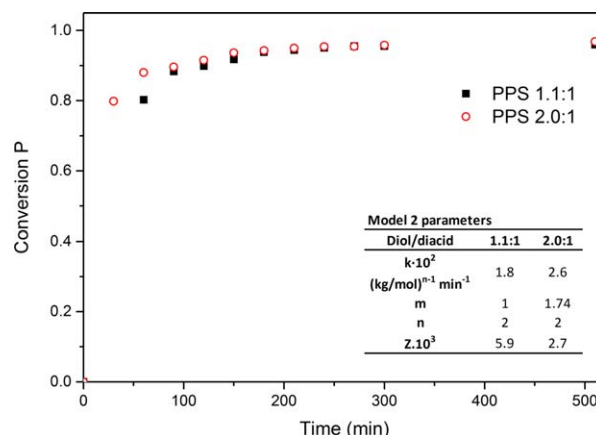


FIGURE 3 Conversion of COOH groups versus time for PPS diol:diacid 1.1:1 and 2:1 at 220 °C and fitted parameters for model 2. [Color figure can be viewed in the online issue, which is available at wileyonlinelibrary.com.]

low as 1.1. Figure 3 shows PPS polymerizations carried out with 1.1:1 and 2:1 diol:diacid molar ratios at 220 °C. The polymerization with 2:1 ratio was as expected to be faster, in agreement with Park et al. observations.⁴⁵ Final acid conversions reached were 96% and 97%. The ratio of 1.1:1 was preferred as it promotes higher molecular weights. For the polymerizations containing both FDCA and SA, optimal diol:diacid ratio was chosen as 1.5:1 which allowed processability of all systems.

It is worth mentioning that the reaction needs to be carefully controlled and cannot be left for reaction times higher than 8 hours as some hot spots can appear and gelling can occur. Acid value determination becomes impossible to perform as samples are insoluble in the titration solvent.

Influence of Temperature and Composition on Rate and Final Conversion

We first studied the synthesis of polyesters containing one of the two diacids. In the case of PPF, both higher final conversion and higher initial rates were achieved as the process temperature was increased, Figure 4. At 230 °C, the conversion reached approximately 80% after the first hour of reaction, while it took about 3 hours to achieve the same conversion at lower temperatures. After 330 minutes of reaction, the conversion reached 96% at 230 °C and 94% at 210 °C.

Interestingly, the PPS polyesters exhibited an almost opposite response to temperature compared to their furan counterparts, as displayed in Figure 4. The highest conversions, 98 and 97%, were achieved at 210 °C and 220 °C, with no significant difference in the kinetic plots between the two process temperatures. At 230 °C the rate of reaction was significantly lower and the final conversion reached was only 94%. We believe that these drops in rate and conversion observed at 230 °C could be attributed to the proximity of the boiling point of succinic acid at 235 °C creating a competition between reaction and evaporation/refluxing. Indeed,

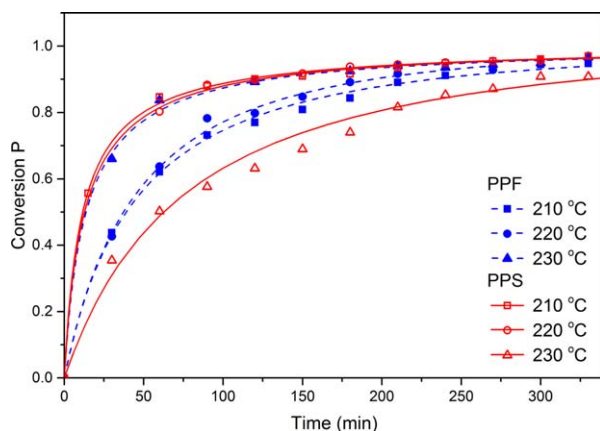


FIGURE 4 Conversion of COOH groups during the polymerization of PPF and PPS at different temperatures fitted to Model 2. [Color figure can be viewed in the online issue, which is available at wileyonlinelibrary.com.]

some crystallization of succinic acid was observed on the glass walls of the reactor supporting this hypothesis.

When comparing the polymerizations of both diacids, we found that the polymerization of FDCA at 230 °C had a similar rate and final conversion to succinic acid polymerized at 210 or 220 °C. This demonstrates that FDCA requires more energy than succinic acid to achieve similar results which will be further discussed in the activation energy section. While increasing temperature is beneficial for the polymerizations containing FDCA it can promote side reactions leading to colouring and appears detrimental to succinic acid polymerization.

Polymerizations with compositions containing both bioderived monomers, succinic acid and FDCA, were also studied. The formation of polyesters was confirmed by ^1H NMR and GPC measurements. Figure 5 shows the ^1H NMR spectra at different time points for PPFPS 50/50 at 220 °C. At the clear point ($t = 0$ h) and in the beginning of the polymerization, when all monomers have been solubilized, peaks for the unreacted 1,3-propanediol are distinguishable at chemical shifts of 3.8 ($\text{CH}_2\text{-OH}$) and 1.8 ppm ($\text{CH}_2\text{-CH}_2\text{OH}$). As the synthesis progresses, unreacted 1,3-propanediol peaks decrease and formation of single or dual-side reacted diols is observed. The peak for the methylene protons on the central carbon shifts depending on the number and type of ester groups resulting in five visible peaks. The signals corresponding to the protons adjacent to the succinic acid ester and FDCA ester group (4.2 and 4.4 ppm, respectively) become more intense by the end of the polyesterification, at 6 and 7 hours. The signals of the succinic acid and FDCA protons correspond to the shifts at 2.6 and 7.2, respectively.

Figure 6 shows the GPC chromatograph for the syntheses at 220 °C. The multiple narrow peaks at high retention times are indicative of the mainly oligomeric nature of polymer. The molecular weight of the polyesters is low and depends on the

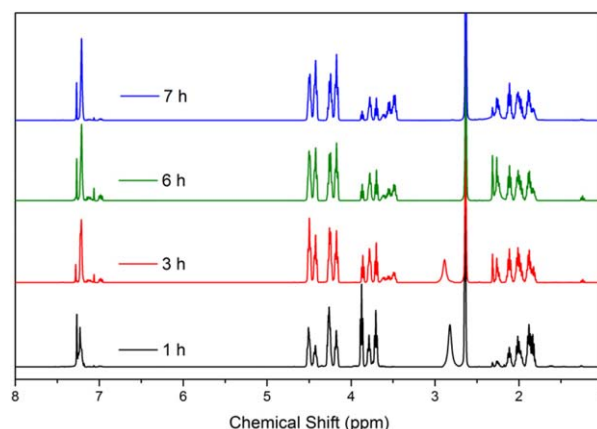


FIGURE 5 ^1H NMR spectra of PPFPS 50/50 polymerization at varying reaction times. [Color figure can be viewed in the online issue, which is available at wileyonlinelibrary.com.]

FDCA/SA composition with higher molecular weights as SA content increases, except for PPFPS 50/50. The chromatograms for PPS and PPFPS 50/50 present broader curves with lower retention times corresponding to higher molecular weights.

Final molecular weights determined by GPC and theoretical values calculated from conversion are provided in Supporting Information for PPS and all PPFPS copolymers, Supporting Information Table S8. Unfortunately PPF was not soluble in THF and no molecular weight values are available. The measured molecular weights were in good agreement with predicted values for SA rich polymers, for PPFPS 30/70 at 220 °C 840 Da by GPC versus 740 Da in theory. We found the molecular weights for FDCA rich polymers were higher than expected, PPFPS 70/30 at 220 °C 1400 Da by GPC versus 840 Da in theory. As the excess diol is limiting the molecular weight of the polymers higher molecular weight values than expected would indicate that the polymerization proceeded further in the polycondensation and excess diol was removed.

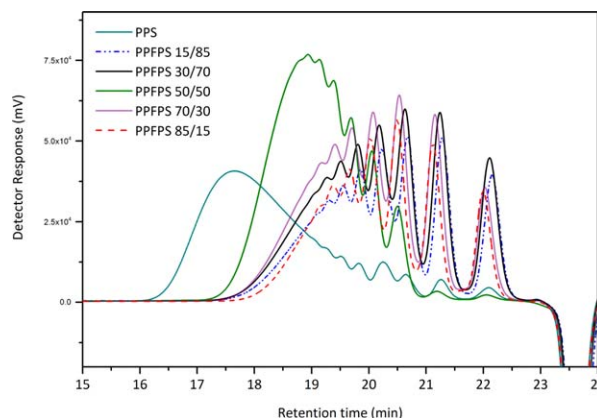


FIGURE 6 Gel permeation chromatography of polymers prepared at 220 °C. [Color figure can be viewed in the online issue, which is available at wileyonlinelibrary.com.]

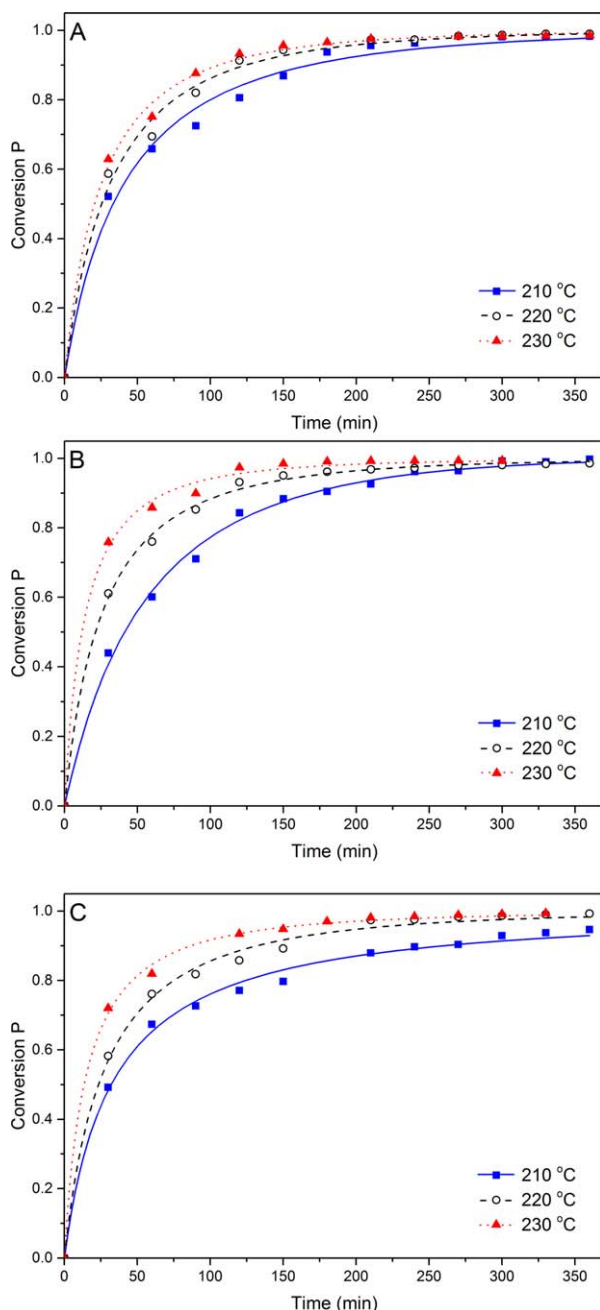


FIGURE 7 Conversion of COOH groups versus time at different temperatures fitted to Model 2 for PPFPS (A) 15/85, (B) 30/70, and (C) 50/50. [Color figure can be viewed in the online issue, which is available at wileyonlinelibrary.com.]

Figures 7 and 8 show the influence of temperature on conversion plots for all PPFPS compositions. It was found that for all copolyesters increasing process temperature resulted in both an increase in the rate of polymerization and in the final conversion, Figures 7 and 8. The extent to which the change in temperature affected rate and final conversion was not consistent through all compositions. For PPFPS 15/85 rates and final conversions at 220 and 230 °C are close, Figure 7(A), while for PPFPS 70/30 the polymerizations at

210 and 220 °C have similar rates and the greatest change occurs between 220 and 230 °C, Figure 8(A).

At 210 °C the final conversions of all the different acid ratios polyesters are above 95% after 350 minutes, however, it is expected that higher conversions could be achieved if the reactions were allowed to proceed for longer times as the trends suggest in Figure 9(A). At the process temperature of 210 °C, the final conversion was generally lower for polymers containing the highest ratios of FDCA.

At 220 °C, Figure 9(B), conversion rates followed a trend with the composition of the PPFPS systems with FDCA rich systems having the lowest initial rate and succinic acid rich one having the highest. The difference in final conversion is less significant at 220 °C than at 210 °C and at 230 °C, all copolyesters reached a conversion of around 99% before 350 min of reaction time, Figure 9(B,C).

At 230 °C, PPFPS 15/85 showed the slowest initial reaction rate of the copolyesters, Figure 9(C). This is in agreement with our prior observations in the synthesis of PPS, whereby temperatures higher than 220 °C reduced the reaction rate. The same effect seems apparent for the copolyester containing the highest relative ratio of succinic acid.

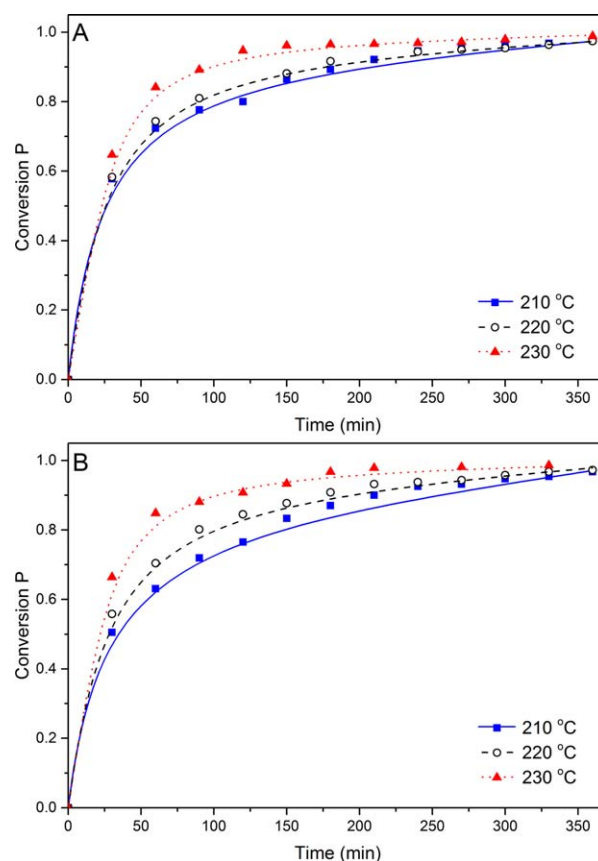


FIGURE 8 Conversion of COOH groups versus time at different temperatures fitted to Model 3 for PPFPS (A) 70/30 and (B) 85/15. [Color figure can be viewed in the online issue, which is available at wileyonlinelibrary.com.]

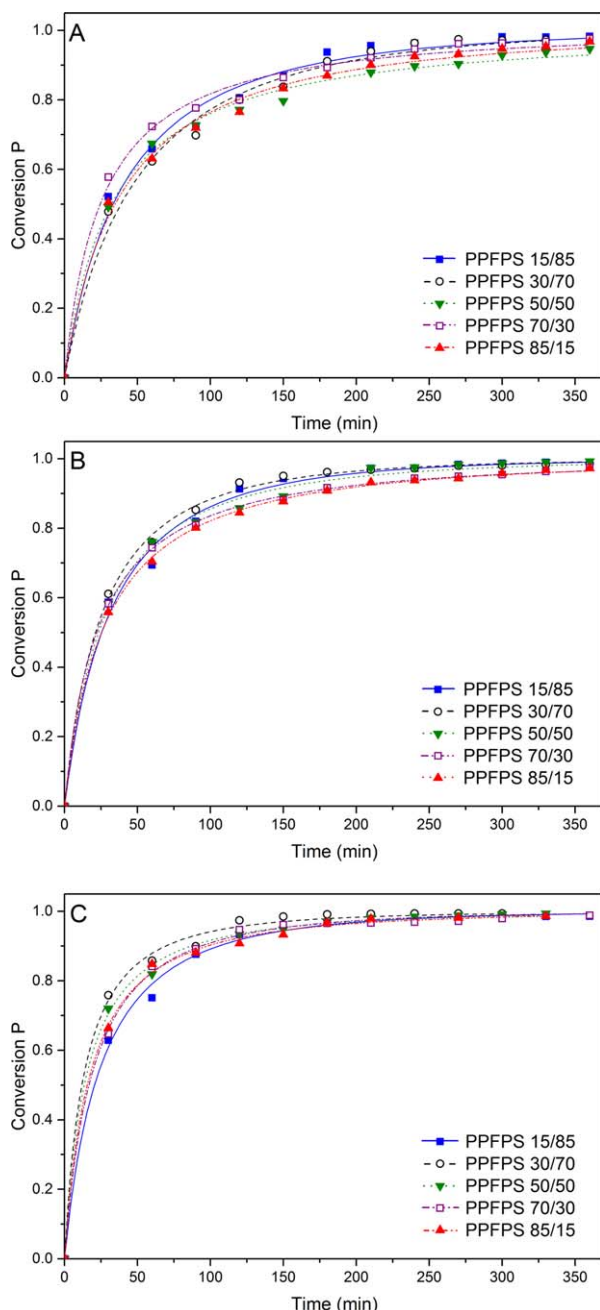


FIGURE 9 Conversion of COOH groups versus time for all monomer compositions fitted to Model 2 at (A) 210 °C, (B) 220 °C, and (C) 230 °C. [Color figure can be viewed in the online issue, which is available at wileyonlinelibrary.com.]

All monomer compositions could be successfully polymerized via the two-step polyesterification process at temperatures of 210 to 230 °C with final conversions for PPFPS polymers between 95% and 99%.

Polyesterification Reaction Modeling

Three models were tested to fit the acid value data for the polymerizations of 1,3-propanediol with FDCA, succinic acid, and mixtures of both diacids. These models were chosen as they represent a progression in the number of parameters

taken into account in the rate equations. Each model's application is limited because of assumptions made when defining variables and key parameters. The main assumption made in Model 1, stoichiometric amounts of diol to diacid, differ from our own experimental conditions of 1.6:1 for PPF, 1.5:1 for PPFPS and 1.1:1 for PPS. In Model 2, all water is considered to be removed from the polymerization medium which is not guaranteed in our system. Finally Model 3 takes into account variations in the properties of the reaction medium and potential ester hydrolysis due to leftover water.

All acid values, C and p values used in this study are available in Supporting Information Tables S1–S5 to allow for direct comparison of our results with other monomer systems or when new models are developed. The best results of the kinetic parameter optimization with the proposed models are summarized in Tables 2 and 3. The Z factor accounts for the numerical value of the least squares minimization objective function. A comparison of Z values allows for the determination of best fit parameters as a lower Z value suggests that the objective function has been better minimized.

As depicted in Table 1, various molar ratios of bio-derived acids were used for the copolyesters synthesized. The experimental data is satisfactorily fitted throughout all the reaction time for all the molar ratios, up to high conversions. In general, the simulation results suggest that the temperature range between 210–230 °C is adequate for the polycondensation process.

Fitting issues were observed around $p = 0.8$ in a number of polymerizations. This was particularly visible at 210 °C, Figure 9(A), and is thought to be due to the experimental set-up change from stage 1 to stage 2 which resulted in a drop in the temperature of the system. Recovery to the desired process temperature was much quicker at 220 °C and 230 °C resulting in less obvious deviations of conversion data points, Figure 9(B,C).

Although the deviation appears more pronounced at 210 °C, Z values are not systematically higher at this temperature and the fitting of the models is still considered satisfactory.

We found that Model 1 and Model 2 provided very similar fits to the data with slightly lower Z values overall for Model 2, Table 2. Model 3 represented an improved fit in particular at higher conversions for FDCA-rich systems, Figure 10.

Generally the reaction order in acid was found to be between 1 and 2 which corresponds to other reported studies.^{34,36,46–48} Several studies suggested that the reaction order for the diacid changes during polymerization and that the overall order of reaction can be fractional as it is a composite of multiple processes.^{48,49} The apparent orders of reaction estimated with Models 1 and 2 were determined by the best fit between the given rate equation and the experimental data and differ from the theoretical or true values. Experimental reaction order and stoichiometry do not represent the same concept. Molecularity refers to the reaction

TABLE 2 Optimization of Kinetic Parameters with Proposed Models 1 and 2

Polyester	<i>T</i> (°C)	Model 1			Model 2			
		$k \times 10^2$, (kg/mol) ^{<i>n</i>-1} min ⁻¹	<i>n</i>	$Z \times 10^3$	$k \times 10^2$, (kg/mol) ^{<i>n</i>-1} min ⁻¹	<i>m</i>	<i>n</i>	$Z \times 10^3$
PPS 1.1	210	2.6	2.0	43.0	2.1	1.2	2.0	12.0
	220	1.8	1.8	9.7	1.8	1.0	2.0	5.9
	230	1.8	1.5	2.2	2.0	0.86	2.0	1.8
PPFPS 15/85	210	3.0	1.4	0.5	2.5	1.1	2.0	0.3
	220	4.0	1.4	1.6	4.0	1.16	2.0	1.3
	230	4.8	1.4	0.6	4.5	1.2	2.0	0.8
PPFPS 30/70	210	3.0	1.2	20.0	2.5	0.93	2.0	1.4
	220	4.0	1.6	0.3	3.5	1.3	2.0	2.0
	230	7.9	1.7	1.7	7.5	1.5	2.0	1.5
PPFPS 50/50	210	4.0	1.9	1.8	2.4	1.7	2.0	1.5
	220	4.1	1.5	2.4	3.4	1.2	2.0	1.7
	230	7.2	1.5	2.5	3.0	1.2	2.0	1.8
PPFPS 70/30	210	4.4	1.8	4.1	3.6	1.5	2.0	3.3
	220	4.9	1.7	0.4	4.1	1.47	2.0	0.2
	230	7.3	1.0	0.3	6.6	1.4	2.0	2.7
PPFPS 85/15	210	3.0	1.7	3.7	2.4	1.3	2.0	2.7
	220	4.3	1.7	0.6	3.6	1.4	2.0	0.3
	230	6.1	1.6	1.9	5.3	1.28	2.0	1.8
PPF	210	3.1	1.6	0.8	2.5	1.3	2.0	0.6
	220	3.4	1.5	0.3	3.0	1.3	2.0	0.3
	230	10.0	1.9	0.6	8.0	1.7	2.0	0.7

mechanism whereas reaction order pertains to an experimental specific rate equation. The reaction order only coincides with the molecularity for elementary reactions that occur in the standard form, $aA + bB \rightarrow cC + dD$. Reaction orders of 1–3 are only found for elementary reactions. With models 1 and 2, the fractional orders are an indication of a series of molecules interacting with active species in the reaction media giving place to the formation of a system with multiple reactions: esterification, polycondensation and ester interchange reactions with the polymer but also with end and bound segments.^{50,51} Approaches such as the transition state theory allow the theoretical determination of true kinetic parameters of a series of elementary steps in particular reaction schemes through the formation of activated complexes. However, the use of this computational chemistry tool is beyond the scope of this study.

Parameter α takes into account the variation of the dielectric constant of the reaction medium during polymerization. In general, in polyesterification reactions the dielectric constant of the reaction mixture decreases as conversion increases. Chen and Wu reported values of α of 0.61, 0.40 and 0.23 for the uncatalyzed adipic acid-ethylene glycol system at 180, 160 and 140 °C, respectively.⁴⁵ Accordingly, parameter α was also found to increase with increasing temperature but the range of values observed was much greater in our case. As

the monomers, which provide the dielectric constant of the medium, are consumed faster at higher temperatures, it is expected α should follow a similar trend. Interestingly the highest value for α for PPS was achieved at 210 °C (1.7), whereas for PPF a higher value for α (2.4) was estimated for the process at 230 °C.

Estimation of Activation Energy

The activation energy (*E_a*) was estimated for the polyesters synthesized at the different process temperatures. The values of the kinetic rate coefficients were plotted against 1/*T* (Absolute temperature, K) to prepare an Arrhenius plot of ln *k* vs 1/*T*. The activation energy was computed from the values of a gradient obtained by least square method and an intercept. The Arrhenius equation explains the reaction rate coefficient as a function of temperature, and it is defined as in eq 12:⁵²

$$k(T) = Ae^{-E_a/RT} \quad (12)$$

Where *A* is the frequency factor, *E_a* is the activation energy (J/mol), *R* is the universal gas constant (8.314 J/mol K) and *T* is the absolute temperature (K). The Arrhenius plot of the polyesterification rate constants of the different systems analyzed is displayed in Figure 11. Table 4 presents the

TABLE 3 Optimization of Kinetic Parameters with Model 3

Polymer	Model 3			
	$T (^{\circ}\text{C})$	$kK_{\text{e0}} \times 10^2$	$k_{\text{h}}[\text{H}_2\text{O}] \times 10^4$	α
PPS 1.1	210	0.5	1.2	1.70
	220	4.8	11.4	0.60
	230	5.9	11.0	0.23
PPFPS 15/85	210	5.8	7.0	0.42
	220	10.6	5.9	0.75
	230	14.6	2.0	1.43
PPFPS 30/70	210	3.3	7.4	1.25
	220	6.4	63.0	0.72
	230	9.6	33.0	0.35
PPFPS 50/50	210	3.8	1.8	0.95
	220	3.7	8.7	1.70
	230	4.0	5.4	1.30
PPFPS 70/30	210	4.1	4.0	0.69
	220	3.8	2.5	1.40
	230	8.7	2.7	2.80
PPFPS 85/15	210	4.1	6.5	0.12
	220	4.2	3.7	1.10
	230	4.6	0.3	2.60
PPF	210	4.0	4.0	1.20
	220	6.4	2.2	2.00
	230	3.9	2.2	2.40

comparison between the activation energies obtained for the various copolymer compositions.

In the case of PPF, the estimated E_{a} is 183.4 kJ/mol which is in good agreement with the estimated value previously reported, 184.3 kJ/mol, for the esterification of PEF synthesis.⁴³ The activation energy for PPS was estimated to be 44.7 kJ/mol. Bikiaris³⁹ reported the activation energies of transesterification and esterification for PPS to be 68.3 and 52.0 kJ/mol, respectively, with a diol:diacid molar ratio of 1.2 and tetrabutoxytitanium as catalyst. Our value is again close to that of the esterification step but the difference in E_{a} is somewhat surprising considering that in our studies we did not utilise a catalyst.

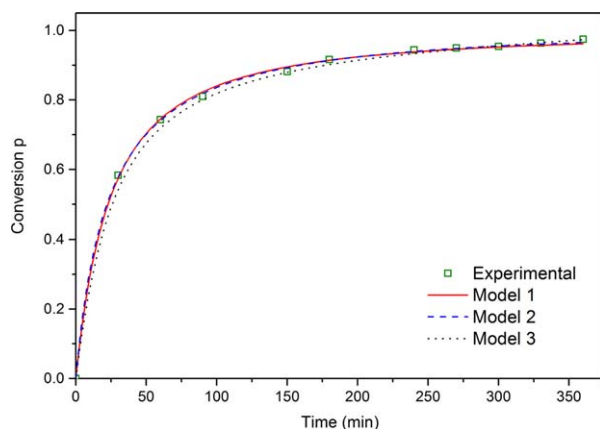


FIGURE 10 Conversion of COOH groups versus time for PPFPS 70/30 at 220 °C fitted with all three models. [Color figure can be viewed in the online issue, which is available at wileyonlinelibrary.com.]

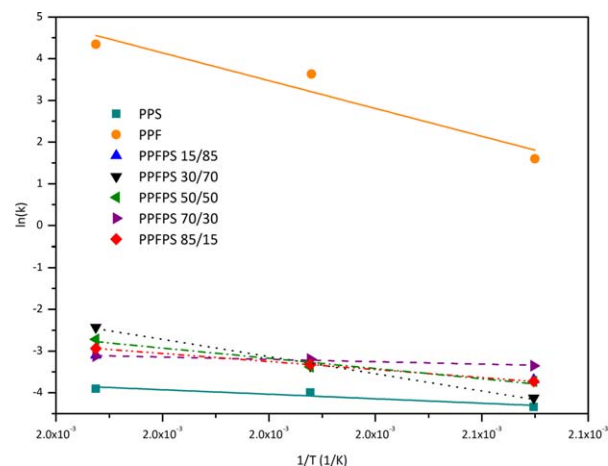


FIGURE 11 Arrhenius Plot for biomass derived polyesters. [Color figure can be viewed in the online issue, which is available at wileyonlinelibrary.com.]

There are several parameters which could explain or contribute to the high Activation Energy observed for PPF compared to PPS. It should be noted that if the rate limiting step of the polyesterification was only dependent on the amount of protons in solution then FDCA should have a faster polymerization than SA as $\text{pK}_{\text{a}1}$ for FDCA is 2.6 while $\text{pK}_{\text{a}1}$ for SA are 4.21. Under acidic conditions, nucleophilic acyl substitution takes place through the protonation of the carbonyl group, activating it for the substitution.⁵³ In the case of FDCA, we propose two processes which could lower the reactivity of the carbonyl carbon. First electron donation of the oxygen of the furan ring to the carbonyl carbon makes it less δ^+ which could lead to reduced reactivity.⁵⁴ Second the positive charge of the protonated carbonyl group is delocalized through mesomeric structures which makes the carbonyl carbon less δ^+ . We propose a mechanism in Supporting Information Figure S5 showing how the formation of these mesomeric

TABLE 4 Estimated Activation Energies by Arrhenius Plots

Polyester	Activation Energy (E_{a} , kJ mol ⁻¹)	R^2
PPS	44.7	0.91
PPFPS 15/85	59.6	0.95
PPFPS 30/70	172.2	0.99
PPFPS 50/50	102.0	0.96
PPFPS 70/30	63.9	0.92
PPFPS 85/15	80.0	1.00
PPF	183.4	0.99

structures would compete with the nucleophilic attack from the alcohol on the carbonyl carbon slowing down what is already the rate limiting step in the process. For succinic acid, there are no mechanisms by which the carbonyl carbon is made less reactive by reduction of the δ^+ .

It should be noted that other factors may contribute to the high activation energy for PPF. FDCA has a high dielectric constant which can limit its solubility in the reaction medium.⁵⁵ As FDCA is only just solubilized in the reaction medium under polymerization conditions, polymerization mixtures containing FDCA have higher viscosities than those with succinic acid only. Reduced diffusion of end groups could lead to a reduction in rate. Finally, although a small contributing factor, reverse polyesterification is greater for stronger acids which would make the ester products from FDCA more prone to hydrolysis than those of succinic acid.⁵⁶

Our calculations indicate that the activation energies of the FDCA polyesters are larger than their succinic acid counterparts for all the ratios explored.

CONCLUSIONS

Biomass-derived polyesters based on 1,3-propanediol, 2,5-furandicarboxylic acid and succinic acid were successfully synthesized at a range of temperatures and with a range of compositions. To the best of our knowledge, this is the first time that these kinetic models and the data obtained have been presented for FDCA biobased polyesters. Moreover, significant experimental and process findings were accomplished. It was found that a preliminary step of mechanical mixing of the diol and 2,5-furandicarboxylic acid followed by heating before the addition of succinic acid overcame the diffusion limitation provoked by the poor solubility of FDCA. GPC and ^1H NMR confirmed the formation of polyesters. As expected, the polymerization rate of FDCA polyesters and copolyesters increased with temperature for most compositions. However, we found the rate of polymerization of succinic acid decreased at 230 °C, which we attributed to competition of monomer evaporation and polymerization. All monomer compositions could be successfully polymerized via the two-step polyesterification process at temperatures 210 to 230 °C with final conversions for PPFPS polymers between 95% and 99%. All polymerizations were modeled using three models with increasing complexity. Model 3 was found to provide better fit for polymerizations with high FDCA contents. Calculated kinetic parameters were in agreement with reported values. Models 1-3 serve as a general screening and will be used as initial estimates for further process simulation work. This work represents a novel and valuable industrial reference for a variety of biomass based polyesterifications, providing practical and useful data in the area of polymerization processing. The study of the influence of molar ratio on the final polymer properties is currently under way.

ACKNOWLEDGEMENTS

All authors are grateful to the Centre for Materials Discovery (CMD) and the Microbiorefinery (MBR) for access to high-throughput synthesis and characterization instrumentation, the EPSRC for financial support (grants EP/K014773/1 and EP/K503952/1) and the U.K. Department for Business Skills and Innovation (Regional Growth Fund, MicroBioRefinery project). They would also like to thank Susan Willis, Cian Bartlam, Omer Erdemli and Chris Lowe from Becker Coating Ltd. for their valuable support. They would also like to thank Dr Rebecca Greenaway, University of Liverpool, for valuable Organic Chemistry conversations. M. Lomeli-Rodríguez is grateful to Consejo Nacional de Ciencia y Tecnología (CONACYT); Secretaría de Educación Pública (SEP).

REFERENCES AND NOTES

- 1 S. Naik, V. V. Goud, P. K. Rout, A. K. Dalai, *Renewable Sustainable Energy Rev.* **2010**, *14*, 578–597.
- 2 A. Mohanty, M. Misra, L. Drzal, *J. Polym. Environ.* **2002**, *10*, 19–26.
- 3 C. Vilela, A. F. Sousa, A. C. Fonseca, A. C. Serra, J. F. Coelho, C. S. Freire, A. J. Silvestre, *Polym. Chem.* **2014**, *5*, 3119–3141.
- 4 A. Peacock, A. Calhoun, *Polymer Chemistry: Properties and Applications*. Hanser Gardner Publications: Munich, **2006**.
- 5 J. V. Kurian, *J. Polym. Environ.* **2005**, *13*, 159–167.
- 6 M. Emptage, S. Haynie, L. Laffend, J. Pucci, G. Whited. *Patent Int. Appl. WO 01/12833 A2*. **2001**.
- 7 J. Xu, B.-H. Guo, In *Plastics from Bacteria*; G. Guo, Q. Chen, eds., Springer-Verlag, Berlin, **2010**, pp 347–388.
- 8 J. J. Bozell, G. R. Petersen, *Green Chem.* **2010**, *12*, 539–554.
- 9 O. Casanova, S. Iborra, A. Corma, *ChemSusChem*. **2009**, *2*, 1138–1144.
- 10 T. Pasini, M. Piccinini, M. Blosi, R. Bonelli, S. Albonetti, N. Dimitratos, J. A. Lopez-Sanchez, M. Sankar, Q. He, C. J. Kiely, *Green Chem.* **2011**, *13*, 2091–2099.
- 11 S. Albonetti, T. Pasini, A. Lolli, M. Blosi, M. Piccinini, N. Dimitratos, J. A. Lopez-Sanchez, D. J. Morgan, A. F. Carley, G. J. Hutchings, *Catalysis Today* **2012**, *195*, 120–126.
- 12 Y. Y. Gorbaney, S. Kegnæs, A. Riisager, *Topics Catalysis* **2011**, *54*, 1318–1324.
- 13 S. E. Davis, L. R. Houk, E. C. Tamargo, A. K. Datye, R. J. Davis, *Catalysis Today* **2011**, *160*, 55–60.
- 14 H. Ait Rass, N. Essayem, M. Besson, *ChemSusChem*. **2015**, *8*, 1206–1217.
- 15 T. Miura, H. Kakinuma, T. Kawano, H. Matsuhisa. U. S. *Patent, US-7411078*; **2008**.
- 16 J. N. Chheda, Y. Román-Leshkov, J. A. Dumesic, *Green Chem.* **2007**, *9*, 342–350.
- 17 T. Ghosh, K. Mahajan, S. Narayan-Sarathy, M. N. Balgacem, P. Gopalakrishnan. U. S. *Patent, US20130171397A1*; **2013**.
- 18 J. Moore, J. Kelly, *Macromolecules* **1978**, *11*, 568–573.
- 19 A. Gandini, A. J. Silvestre, C. P. Neto, A. F. Sousa, M. Gomes, *J. Polym. Sci. Part A: Polym. Chem.* **2009**, *47*, 295–298.
- 20 P. Gopalakrishnan, S. Narayan-Sarathy, T. Ghosh, K. Mahajan, M. N. Balgacem, *J. Polym. Res.* **2014**, *21*, 1–9.
- 21 M. Jiang, Q. Liu, Q. Zhang, C. Ye, G. Zhou, *J. Polym. Sci. Part A: Polym. Chem.* **2012**, *50*, 1026–1036.
- 22 G. Z. Papageorgiou, V. Tsanaktsis, D. G. Papageorgiou, S. Exarhopoulos, M. Papageorgiou, D. N. Bikiaris, *Polymer* **2014**, *55*, 3846–3858.

- 23 J. Ma, Y. Pang, M. Wang, J. Xu, H. Ma, X. Nie, *J. Mater. Chem.* **2012**, *22*, 3457–3461.
- 24 A. Sousa, A. Fonseca, A. Serra, C. Freire, A. Silvestre, J. Coelho, *Polym. Chem.* **2016**, *7*, 1049–1058.
- 25 P. J. Flory, *J. Am Chem Soc* **1939**, *61*, 3334–3340.
- 26 E. Szabo-Rethy, *Eur Polym J* **1971**, *7*, 1485–1499.
- 27 T. Yamada, Y. Imamura, O. Makimura, *Polym. Eng. Sci.* **1985**, *25*, 788–795.
- 28 C. K. Kang, B. C. Lee, D. W. Ihm, *J. Appl. Polym. Sci.* **1996**, *60*, 2007–2015.
- 29 K. Ravindranath, R. Mashelkar, *Chem. Eng. Sci.* **1986**, *41*, 2969–2987.
- 30 H. Patel, G. Feix, R. Schomäcker, *Macromol React Eng.* **2007**, *1*, 502–512.
- 31 P. Zetterlund, W. Weaver, A. Johnson, *Polym. React Eng.* **2002**, *10*, 41–57.
- 32 M. Shah, E. Zondervan, A. de Haan, *Polym. Eng. Sci.* **2011**, *51*, 2495–2504.
- 33 R. Jedlovčnik, A. Šebenik, J. Golob, J. Korbar, *Polymr. Eng. Sci.* **1995**, *35*, 1413–1417.
- 34 T. Salmi, E. Paatero, P. Nyholm, M. Still, K. Na, *Chem. Eng. Sci.* **1994**, *49*, 5053–5070.
- 35 K. Nalampang, A. Johnson, *Polymer* **2003**, *44*, 6103–6109.
- 36 A. Fradet, E. Maréchal, In *Polymerizations and Polymer Properties*; Springer-Verlag, **1982**, pp 51–142.
- 37 K. Seavey, Y. A. Liu, *Step-Growth Polymerization Process Modeling and Product Design*; John Wiley & Sons: New York, **2009**.
- 38 D. N. Bikiaris, D. Achilias, *Polymer* **2006**, *47*, 4851–4860.
- 39 D. Bikiaris, D. Achilias, *Polymer* **2008**, *49*, 3677–3685.
- 40 S. S. Park, H. W. Jun, S. S. Im, *Polym. Eng. Sci.* **1998**, *38*, 905–913.
- 41 M. Garin, L. Tighzert, I. Vroman, S. Marinkovic, B. Estrine, *J. Appl. Polym. Sci.* **2014**, *131*, n/a–n/a.
- 42 L. Hu, L. Wu, F. Song, B. G. Li, *Macromol. React Eng.* **2010**, *4*, 621–632.
- 43 T. Matsuo, M. Kamikawa, T. Kondo, N. Maeda. *Patent US20140024793 A1*, **2013**.
- 44 H. R. Allcock, F. W. Lampe, J. E. Mark, H. Allcock, *Contemporary Polymer Chemistry*; Pearson Education Upper Saddle River: New Jersey, **2003**.
- 45 S. Chen, K. C. Wu, *J. Polym. Sci.: Polym. Chem. Ed.* **1982**, *20*, 1819–1831.
- 46 L. C. G. Fang Yao-Ren, L. U. Jia-Lin, C. H. E. N. Mu-Kuo, *Sci. China Math.* **1975**, *18*, 72–87.
- 47 T. Au-Chin, Y. Kuo-Sui, *J. Polym. Sci.* **1959**, *35*, 219–233.
- 48 T. Salmi, E. Paatero, P. Nyholm, *Chem. Eng. Process* **2004**, *43*, 1487–1493.
- 49 R. Bacaloglu, M. Fisch, K. Biesiada, *Polym. Eng. Sci.* **1998**, *38*, 1014–1022.
- 50 J. J. Carberry, *Chemical and Catalytic Reaction Engineering*; Mineola, N.Y.: Dover Publications, **2001**.
- 51 G. F. Froment, Kenneth B. Bischoff, Juray De Wilde, *Chemical Reactor Analysis and Design*; Wiley: New York, **1990**.
- 52 I. Pomakis, I. Simitzis, *Die Angewandte Makromolekulare Chemie* **1981**, *99*, 145–170.
- 53 C. K. Ingold, *Structure and Mechanism in Organic Chemistry*; Cornell University Press: Ithaca, New York, **1969**.
- 54 J. A. Joule, K. Mills, *Heterocyclic Chemistry*; Chichester: Wiley, **2010**.
- 55 Z. Zhang, J. Zhen, B. Liu, K. Lv, K. Deng, *Green. Chem.* **2015**, *17*, 1308–1317.
- 56 I. Vancsó-Szmercsányi, K. Maros-Gréger, E. Makay-Bödi, *Eur Polym J* **1969**, *5*, 155–161.